Supplementary data for Lim et al.

**Phosphoenolpyruvate depletion mediates both growth arrest and drug tolerance of *Mycobacterium tuberculosis* in hypoxia.**

Juhyeon Lim[†], Jae Jin Lee[†], Sun-Kyung Lee[‡], Seoyong Kim[†], Seok-Yong Eum[‡], Hyungjin Eoh [†,*]

This document contains Supplementary methods and references; Supplementary Figures and legends S Fig. 1 – 16; Supplementary Tables 1 – 2.

Supplementary Methods

**Bacterial strains, culture conditions and chemicals**

Mtb H37Rv, *pckA* deficient (ΔpckA), *tgs1* deficient (Δtgs1), and their complement strains (ΔpckA/com and Δtgs1/com, respectively) were cultured in a biosafety level 3 facility. Mtb H37Rv (ΔleuCDΔpanCD) was cultured in a biosafety level 2+ facility at 37 °C in Middlebrook 7H9 broth (m7H9) or on Middlebrook 7H10 agar (m7H10) (Difco) supplemented with 0.2% acetate (or 0.2% glucose in case of requirement), 0.04% tyloxapol (broth only), 0.5g/L BSA and 0.085% NaCl. Mtb H37Rv (ΔleuCDΔpanCD) was cultured by supplementing with leucine and vitamin B5 (1). Drug-sensitive (DS), Rifampicin mono-resistant (RMR), multidrug-resistant (MDR), and extensively drug-resistant (XDR) and totally drug-resistant (TDR) TB clinical isolates were originally isolated from the sputum of TB patients at the National Masan Tuberculosis Hospital (NMTH). We have compiled all relevant ethical regulations for work with TB clinical isolates. Human specimen collection was approved by the NMTH Institutional Review Board (project licenses: IRB-04-I-N01 and IRB-05-I-M069) and written informed consent was obtained from the patients for collection and use of the specimens for research only. Phosphoenolpyruvate, dimethyl-αKG, TAG, and methylene blue were purchased from Sigma-Aldrich (Saint Louis, MO, USA). Ampicillin and isoniazid were also purchased from Sigma-Aldrich and used at 125 μg/mL (10 X MIC) and 0.03 or 0.3 μg/mL (1X or 10X MIC), respectively.

**Mtb metabolite extraction**

Mtb-laden filters used for metabolomics profiling were generated as previously described (2) and incubated at 37 °C on m7H10 for 5 days to reach the mid-log growth phase. The filters were transferred onto chemically identical m7H10 containing 0.2% $^{12}C$ acetate or [U-$^{13}C$] acetate as the single carbon source. Mtb-laden filters were metabolically quenched by plunging filters into a mixture of acetonitrile:methanol:$H_2O$ (40:40:20) precooled to - 40 °C, and metabolites were extracted by mechanical lysis with 0.1 mm Zirconia beads in a Precellys tissue homogenizer for 4 min (6,800 rpm) twice under continuous cooling at or below 2 °C. Lysates were clarified by centrifugation and then filtered across a 0.22 μm Spin X column. Residual protein content of the metabolite extracts was determined to normalize the samples to cell biomass (BCA protein assay kit, Thermo Scientific). All data obtained by metabolomics were the averages of independent triplicates.

**LC-MS metabolomics profiling**

Liquid chromatography mass spectrometry (LC-MS) based metabolomics was used as previously described (2). Extracted metabolites were separated on a Cogent Diamond Hydride type C column (gradient 3) and the mobile phase consisted of solvent A (dd$H_2O$ with 0.2% formic acid) and solvent B (acetonitrile with 0.2% formic acid). The gradient used was as previously described (2). The mass spectrometer used was an Agilent Accurate Mass 6230 time of flight (TOF) coupled with an Agilent 1290 liquid chromatography (LC) system. Dynamic mass axis calibration was achieved by continuous infusion of a reference mass solution using an isocratic pump with a 100:1 splitter. This configuration achieved mass errors of 5 ppm, mass resolution ranging from 10,000 to 25,000 (over m/z 121 – 966 atomic mass units), and 5 $\log_{10}$ dynamic range. Detected ions were deemed metabolites on the basis of unique accurate mass-retention time identifiers for masses exhibiting the expected distribution of accompanying isotopomers. Metabolites were quantified using a calibration curve generated with chemical standards spiked into homologous Mtb extract (1:10 diluted with metabolite extraction solution) to correct for matrix-associated ion suppression effects. The abundance of metabolites was extracted using Agilent Qualitative Analysis B.07.00 and Profinder B.08.00 software (Agilent Technologies) with a mass tolerance of <0.005 Da. The clustered heatmap, hierarchical clustering, principal component analysis, volcano plot, and pathway enrichment analysis were conducted using MetaboAnalyst (ver. 4.5). All data obtained by metabolomics profiling were the average of at least two independent triplicates.

**Isotopologue analysis using [U-$^{13}$C] acetate**

The extent of isotopic labeling for metabolites was determined by dividing the summed peak height ion intensities of all labeled isotopologue species by the ion intensity of both labeled and unlabeled species, expressed as a percentage. Label-specific ion counts were corrected for naturally occurring $^{13}$C species (i.e., M1, M2, M3 and so on). The relative abundance for each isotopically labeled species was determined by dividing the peak height ion count of each isotopic form by the summed peak height ion count of all labeled species. Ion counts were converted into molar abundances using standard curves generated by chemical standards and serial dilutions to establish the co-linearity of ion counts and molar abundance.

**Bone marrow derived macrophages (BMDM) infection and CFU enumeration assay**

Bone marrow was removed from the femur and tibia of eight- to ten- week-old C57BL/6 mice after euthanasia. Macrophage precursors were differentiated in Dulbecco's modified Eagle medium (DMEM) supplemented with 10% fetal bovine serum, 20% L929 cell-conditioned medium, and 10

ng/mL murine IFN-γ (R&D systems) for 1 day as previously described (3). L929 cell-conditioned medium was used as a source of macrophage colony stimulating factor (M-CSF). A total of 1 X $10^5$ BMDM per well in 96 well plates were replated and exposed to single-cell suspended Mtb harvested from the early log phase of growth at multiplicity of infection (MOI) of 5 or 10. Four hours after infection, BMDM were washed twice with PBS to remove unphagocytosed extracellular bacteria and replaced with fresh medium. Infected BMDM were treated with 30 µg/mL gentamycin overnight to kill the unphagocytosed fraction. Following treatment with INH with or without 10 mM PEP and/or 5 mM αKG, cells were lysed with 0.5% Triton X-100 and released bacilli were counted by plating serial dilutions of the lysate on m7H10 at days 0 and 6 post infection.

### *In vitro* CFU enumeration assay

Mtb viability was determined using liquid cultures manipulated under experimentally identical conditions as filter-grown cultures for metabolomics profiling, which we previously demonstrated to be microbiologically similar (2). CFUs were determined by plating on m7H10 after incubating for at least 3 weeks at 37 °C. To study effects of PEP or antibiotics on hypoxic Mtb viability, we modified our hypoxia chambers by preinstalling with a squeezable, plastic Pasteur pipette loaded with either 10 mM PEP or 10X MIC equivalent INH in a final volume of 500 µL affixed to the roof of the chamber (Fig. S3a). After 24 hrs of hypoxic incubation, PEP and INH were added to the media by squeezing the pipette without breaking hypoxia and further incubated for 18 hrs at 37 °C. Vehicle was used as a control. Then, bacilli were immediately resuspended in 0.04% tyloxapol in PBS. Harvested cultures were vortexed for 1 min with 2 mm glass beads to generate a single cell suspension and CFUs were counted by plating on m7H10 after at least a 3-week incubation at 37 °C. CFU enumeration assays were conducted in two independent triplicates.

### Membrane potential determination

Mtb membrane potential was measured by the BacLight bacterial membrane potential kit (Thermofisher Scientific) as previously described and adapted to our *in vitro* hypoxia apparatus (2). Mtb cultures were grown in complete m7H9 to mid-log phase and concentrated to $OD_{595}$ ~1.0 in m7H9 containing 0.2% acetate after degassing. Mtb cultures were aliquoted and inserted into the hypoxia chamber already preinstalled with a squeezable Pasteur pipette loaded with 15 µM $DiOC_2$ as previously described. After hypoxic incubation, $DiOC_2$ was added and incubated for 20 min at room temperature, followed by fixation with 1% formaldehyde for an additional 10 min.

Cultures were then washed with fresh m7H9 to remove extracellular dye. As a positive control, cultures grown under ambient air were treated with 5 μM of the protonophore carbonyl-cyanide 3-chlorophenylhydrazone (CCCP; Invitrogen). The assay was performed in black with clear-bottom 96 well plates (Costar); green fluorescence (488/530 nm) and shifts to red fluorescence (488/610 nm) were measured. Membrane potential was measured as a ratio of red fluorescence to green fluorescence. Each condition was measured in two independent triplicates.

**Measurement of intrabacterial ATP and NADH/NAD ratios**

Mtb-laden filters used for metabolomics profiling were generated to measure intrabacterial ATP and NADH/NAD. Intrabacterial ATP concentrations were measured using the BacTiter Glo Microbial Cell Viability Assay according to the manufacturer's instructions (Promega). NAD and NADH concentrations were measured using the FluroNAD/NADH detection kit (Cell Technology). Mtb metabolism was rapidly quenched by plunging bacilli in the first solvent in the kit.

**Extraction of RNA and qRT-PCR**

Total RNA was extracted from Mtb-laden filters cultured for hypoxic Mtb metabolomics profiling. Cells were resuspended in 1 mL cold TRIzol (Gibco/BRL), transferred to 2 mL screw-cap tubes containing 0.4 mL 0.1 mm Zirconia beads, and mechanically lysed using a Precellys tissue homogenizer. Lysates were clarified by centrifugation and TRIzol supernatant was used for RNA extraction. RNA was isolated using an Qiagen RNA extraction kit. Isolated RNA was treated with DNase I to remove DNA contamination (Sigma-Aldrich). RNA concentrations were determined using a Nanodrop, and qRT-PCR reactions were conducted using an iQ SYBR-Green Supermix (Bio-Rad) and a C1000$^{TM}$ Thermal Cycler Instrument. Primers used for amplification are listed in Supplementary Table 2. Fold changes were calculated by ΔΔCT values that were normalized to *sigA* transcript levels and depicted as $\log_2$ values.

**Drug uptake measurement**

Our filter culture system was modified by replacing the underlying agar media with a plastic inset containing chemically equivalent m7H9 (with no detergent) in direct contact with the underside of Mtb-laden filters as shown in Fig. S13a. m7H10 and m7H9 contained 10X MIC equivalent INH. Growth atop m7H9 was indistinguishable from that achieved on adjacent m7H10 and enabled timed start-stop measurements of drug uptake by sampling the cell free m7H9. A blank filter was used as a negative control. After a 1-day incubation, cell free m7H9 was collected and INH was

extracted by adding an LC-MS grade acetonitrile:methanol:$H_2O$ (40:40:20) solution that was precooled to – 40 °C and quantified by LC-MS. Total Mtb biomass was determined to normalize the INH ion counts to biomass (BCA protein assay kit, Thermo Scientific).

**Oxygen consumption rate (OCR) measurement**

OCR in Mtb was quantified using the Seahorse XFe96 extracellular flux analyzer (Agilent Technologies) as previously described (4). Briefly, ΔleuCDΔpanCD BSL2+ strains were grown to the stationary phase ($OD_{595}$, ~2.5), washed and resuspended with PBS. Cells were diluted 1:100 ($OD_{595}$, 0.2) and then adhered to poly-d-lysine-coated XFe96 microplates and treated with 20 µL PEP and/or αKG. Basal OCR was measured for 12 min prior to PEP and/or αKG to verify uniform cell adhesion. OCR measurements were acquired at 6 min intervals. Treatment with CCCP was used as a positive control.

**BODIPY FL vancomycin-labeling**

Mtb cultures were incubated in the hypoxia chamber with or without PEP. After 18 hrs of hypoxic incubation, the Mtb culture was harvested and fixed with PBS supplemented with 0.04% tyloxapol and 2.5% glutaraldehyde for an additional 24 hrs. Harvested cells were diluted to $OD_{595}$ 0.4 and incubated with 1 mg/mL of BODIPY FL vancomycin solution (Invitrogen Corp., Carlsbad, CA) for 24 hrs at 37 °C. For microscopic analysis, cells were washed with PBS and imaged on a Zeiss LCM 800 upright confocal system (Carl Zeiss, Oberkochen, Germany). Images were acquired by ZEN software and processed using Image J (1.52) and Photoshop CS6.

**Triacylglycerol extraction**

Total lipid extraction was performed as previously described with minor modifications (5). Lipids were extracted from the Mtb-laden filters that were used for metabolomics profiling. After incubation inside the hypoxia chambers, three filters were combined for each condition to enable a sufficient amount of lipids to be detected by TLC analysis. After collection, cells were washed twice with PBS, transferred to a 50 mL amber glass bottle and treated with 6 mL $CHCl_3$:$CH_3OH$ (2:1, v/v) for sterilization, treated with additional 4 mL $H_2O$, and incubated for 24 hrs at 4 °C. After centrifugation at 3,000 rpm for 20 min, the lower organic phase was isolated and dried under a continuous nitrogen stream. Dried lipids were resuspended in 300 µL $CHCl_3$:$CH_3OH$ (1:1, v/v). Analytical TLC was carried out in Silica 60F254 (Sigma). The mobile phase of TLC analysis used to detect TAG was hexane: diethyl either: formic acid (45:5:1, v/v/v). TLC plates were sprayed

with 10% phosphomolybdic acid and baked at 120°C. The labeled bands shown in the TLC correspond to $R_f$ of TAG standard.

**References**


1. Vilcheze C*, et al.* (2018) Rational Design of Biosafety Level 2-Approved, Multidrug-Resistant Strains of *Mycobacterium tuberculosis* through Nutrient Auxotrophy. (Translated from eng) *MBio* 9(3).
2. Eoh H & Rhee KY (2013) Multifunctional essentiality of succinate metabolism in adaptation to hypoxia in *Mycobacterium tuberculosis*. *Proc Natl Acad Sci U S A* 110(16):6554-6559.
3. Lee JJ*, et al.* (2018) Glutamate mediated metabolic neutralization mitigates propionate toxicity in intracellular *Mycobacterium tuberculosis*. *Scientific Reports* 8(1):8506.
4. Saini V*, et al.* (2016) Ergothioneine Maintains Redox and Bioenergetic Homeostasis Essential for Drug Susceptibility and Virulence of *Mycobacterium tuberculosis*. *Cell Rep* 14(3):572-585.
5. Bligh EG & Dyer WJ (1959) A rapid method of total lipid extraction and purification. *Can J Biochem Physiol* 37(8):911-917.

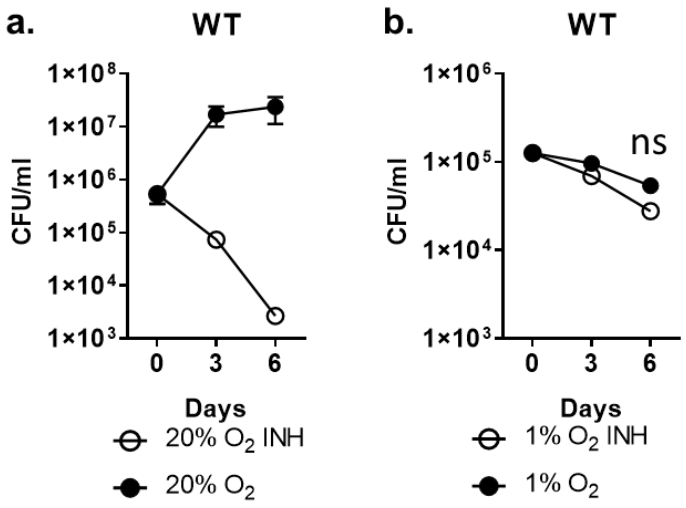


**S Fig. 1. Hypoxic Mtb becomes growth arrested and drug tolerant.** Mtb CFU viability while adapting to 20% $O_2$ (**a**) and to 1% $O_2$ (**b**) in the presence or absence of 10X MIC equivalent amount of INH at days 0, 3, and 6. All values are the average of three biological replicates ± SEM. ns, not significant by Student's unpaired t-test.

a.

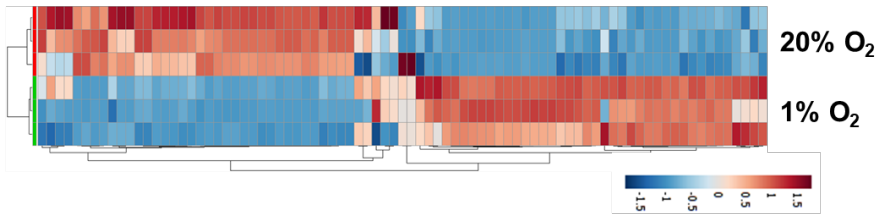


b.

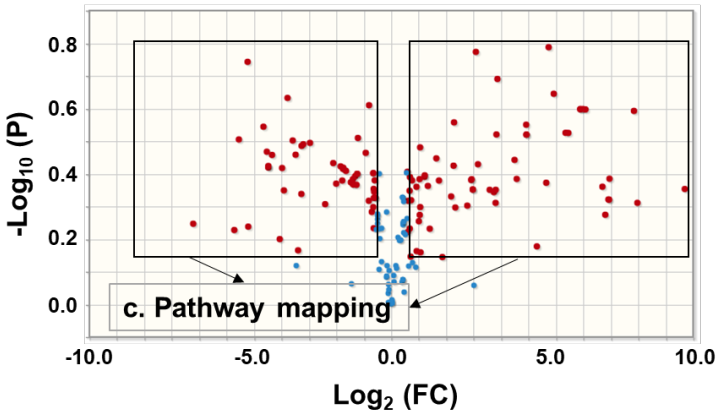


c.

| Rank | Pathway mapping result | *P* value |
|---|---|---|
| 1 | Starch and Sucrose metabolism | 0.01157 |
| 2 | Glutamine-glutamate metabolism | 0.00009 |
| 3 | Ala-Asp-Glu metabolism | 0.00037 |
| 4 | Arg biosynthesis metabolism | 0.00001 |
| 5 | Glycolysis/Gluconeogenesis | 0.00157 |
| 6 | TCA cycle/glyoxylate shunt | 0.01694 |
| 7 | Purine metabolism | 0.11387 |
| 8 | Pyruvate metabolism | 0.00425 |
| 9 | Gly, Ser and Thr metabolism | 0.08634 |
| 10 | Pantothenate and CoA biosynthesis | 0.13667 |

**S Fig. 2. Pathway enrichment analysis of the hypoxic Mtb metabolome**. (**a**) Clustered heatmap depicting levels of ~100 Mtb metabolites of hypoxic Mtb (1% $O_2$) and normoxic Mtb (20% $O_2$) cultured in m7H9 containing 0.2% acetate. Rows depict conditions and columns indicate individual metabolites. Data were parsed using uncentered Pearson's correlation with centroid linkage clustering and rendered using MetaboAnalyst (ver 4.5). Data are depicted on a $\log_2$ scale relative to that of the replicating state. (**b**) Volcano plots of relative abundance of metabolites in hypoxic Mtb vs. normoxic Mtb. FC, fold change. The y-axis indicates $-\log_{10}$[P] and the x-axis shows relative abundance in $\log_2$ scale. Metabolites that are significantly altered in hypoxic Mtb relative to replicating Mtb (red dots) are listed in Supplementary Table 1. (**c**) Pathway enrichment analysis using a subset of metabolites listed in Supplementary Table 1.

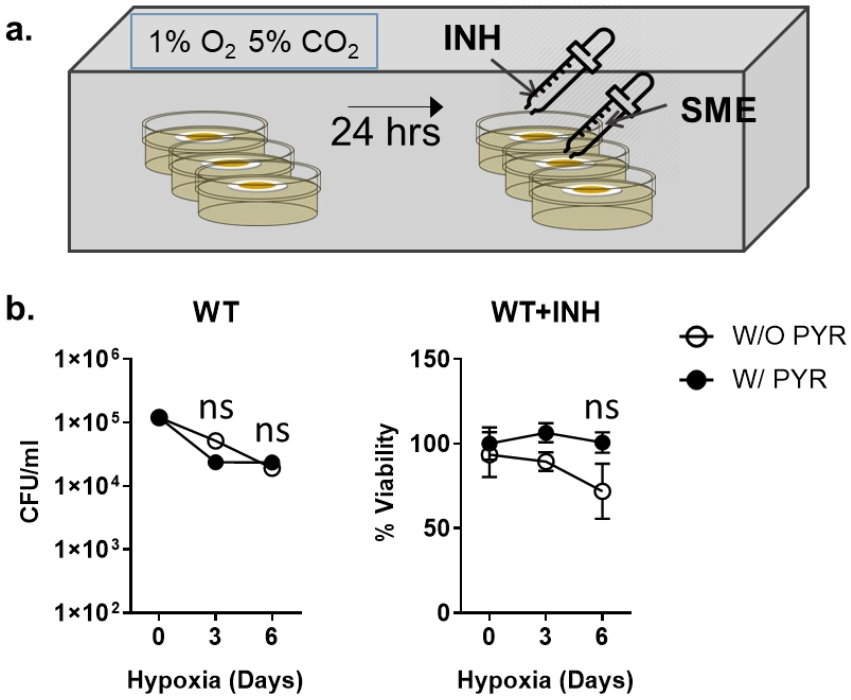


**S Fig. 3. The hypoxia chamber and effect of pyruvate on hypoxic Mtb drug tolerance.** (**a**) The device used to monitor the effect of supplementing with SME or PEP on hypoxic Mtb. The hypoxic chambers are flexible plastic bags that contain squeezable plastic Pasteur pipettes preloaded with degassed medium containing SME or PEP affixed to the roof of the bags. (**b**) The effect of supplementing 10 mM pyruvate on hypoxic Mtb growth (left panel) and INH susceptibility (right panel). Experiments were conducted in m7H9 containing 0.2% acetate. All values are the average of three biological replicates ± SEM. ns, not significant by Student's unpaired t-test.

a.

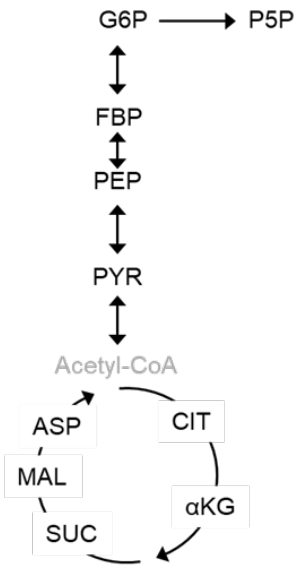


b.

| Metabolites | Normoxia (nmol/mg) | Hypoxia (nmol/mg) | Hypoxia/ Normoxia | P-value |
|---|---|---|---|---|
| PEP | 49.6 ± 5.21 | 4.47 ± 1.03 | 0.09 ± 0.02 | <0.0001 |
| αKG | 41.8 ± 4.96 | 8.20 ± 0.17 | 0.19 ± 0.01 | 0.0003 |
| Pyruvate | 22.2 ± 2.13 | 14.3 ± 2.50 | 0.64 ± 0.11 | 0.014 |
| Citrate | 782.7 ± 26.5 | 711.1 ± 36.8 | 0.90 ± 0.04 | 0.0523 |
| Aspartate | 6.15 ± 2.79 | 6.32 ± 0.16 | 1.02 ± 0.27 | 0.92 |
| Malate | 1.52 ± 0.45 | 5.51 ± 1.41 | 3.60 ± 0.92 | 0.0096 |
| Fumarate | 0.71 ± 0.29 | 3.45 ± 0.54 | 4.82 ± 0.75 | 0.0015 |
| FBP | 16.3 ± 3.77 | 97.8 ± 17.2 | 5.97 ± 1.05 | 0.0013 |
| Succinate | 14.8 ± 8.13 | 164.6 ± 5.61 | 11.0 ± 0.37 | <0.0001 |
| Glucose-P | 9.46 ± 0.51 | 124.0 ± 9.01 | 13.5 ± 0.98 | <0.0001 |
| Pentose-P | 9.16 ± 0.50 | 133.7 ± 14.5 | 14.6 ± 1.58 | 0.0001 |

**S Fig. 4. Intrabacterial concentrations of central carbon metabolism intermediates of hypoxic and normoxic Mtb**. (**a**) Schematic depicting Mtb CCM pathways. G6P, glucose phosphates (Glucose-P); FBP, fructose 1,6 bisphosphates; PEP, phosphoenolpyruvate; PYR, pyruvate; P5P, pentose phosphates (Pentose-P); CIT, citrate; αKG, alpha-ketoglutarate; SUC, succinate; MAL, malate; ASP, aspartate. (**b**) CCM pathway intermediates of hypoxic and normoxic Mtb were quantified using a standard curve generated with a chemical standard. m7H9 media containing 0.2% acetate was used. Metabolites in the table were sorted in descending order of concentration between hypoxia and normoxia.

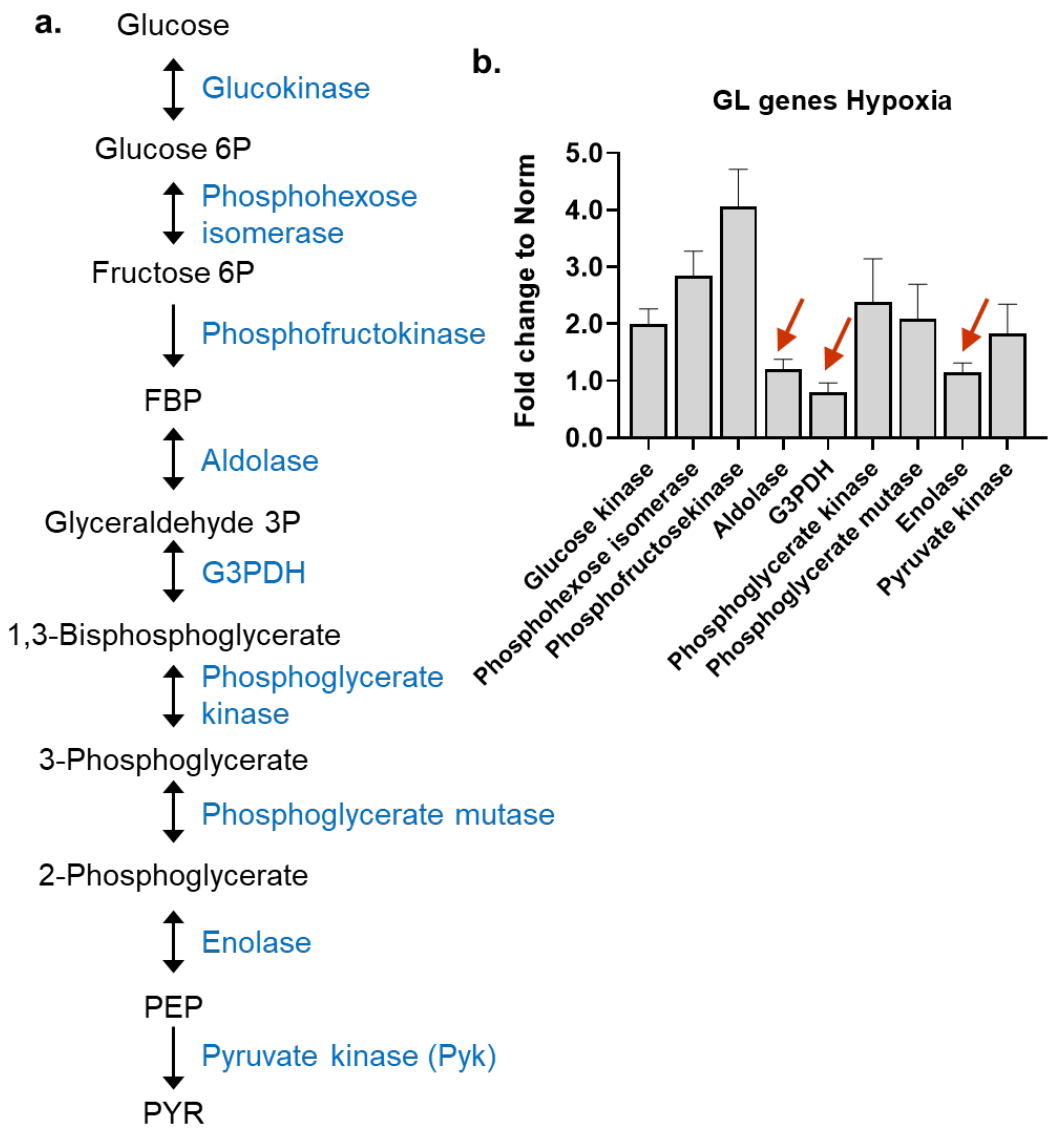


**S Fig. 5. qRT-PCR analysis of targeted genes involved in Mtb glycolysis under hypoxia**. (**a**) Schematic depicting Mtb glycolysis. Blue font, enzyme names; black font, metabolite names. (**b**) Relative mRNA expression levels of Mtb glycolysis genes in hypoxic Mtb as compared to those of normoxic Mtb (Norm). Red arrows indicate the genes with lower mRNA expression as compared to other glycolysis genes under hypoxia. G3PDH, glyceraldehyde 3 phosphate dehydrogenase.

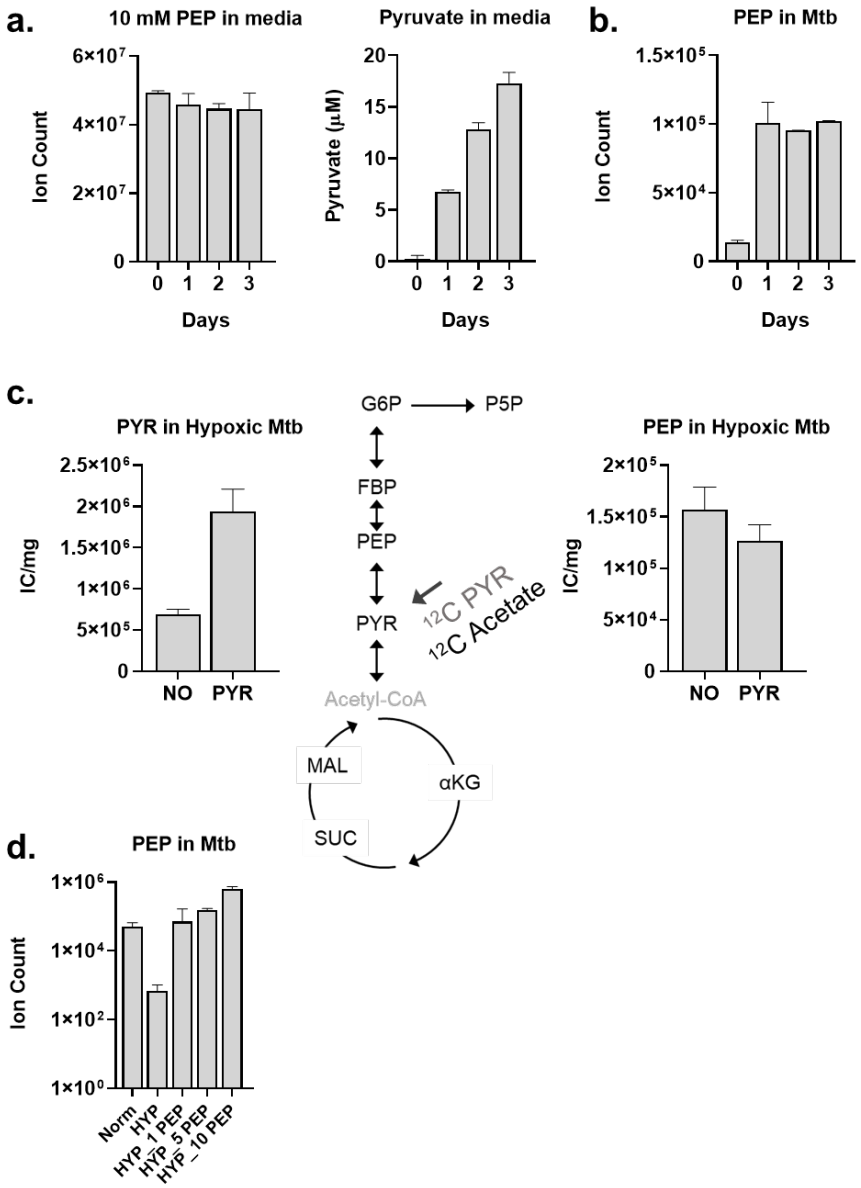


**S Fig. 6. Stability test of PEP chemical standard**. (**a**) LC-MS monitoring the ion count of 10 mM PEP chemical standard and pyruvate amount arising from spontaneous hydrolysis of 10 mM PEP after incubating in m7H9 for 3 days. Pyruvate amount was calculated by generating a standard curve derived from known concentrations of pyruvate chemical standard. (**b**) Intrabacterial PEP levels within hypoxic Mtb after treatment with 10 mM PEP for 3 days. (**c**) Intrabacterial PEP and pyruvate ion counts (IC) of hypoxic Mtb after supplementing with 10 mM pyruvate. The PEP level in hypoxic Mtb was not altered by supplementing with pyruvate. (**d**) Intrabacterial PEP ion counts of normoxic Mtb and hypoxic Mtb, and the effect of supplementing with exogenous PEP (1 – 10 mM) on intrabacterial PEP of hypoxic Mtb.

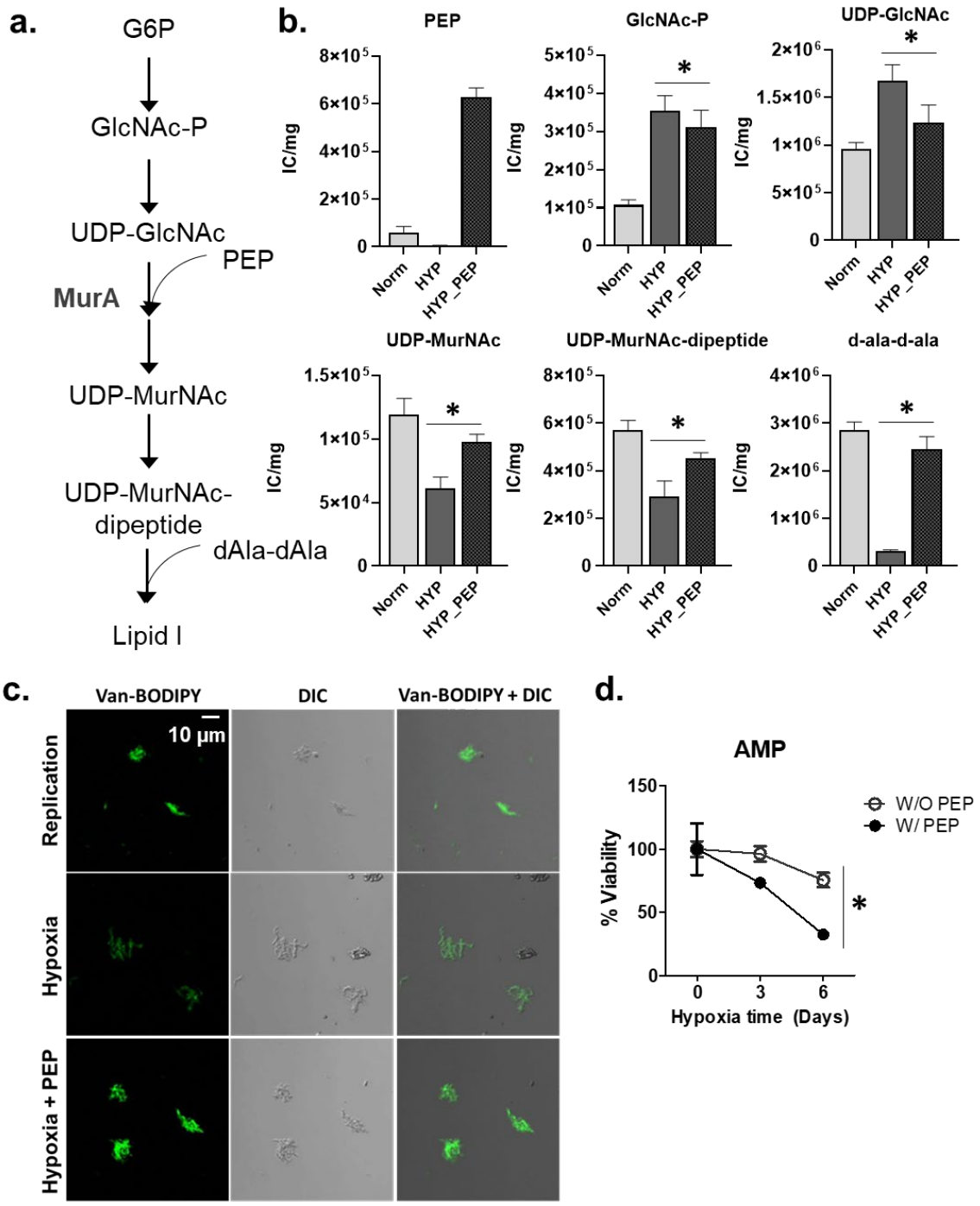
a.
G6P
GlcNAc-P
UDP-GlcNAc
PEP
MurA
UDP-MurNAc
UDP-MurNAc-dipeptide
dAla-dAla
Lipid I
b.
PEP
GlcNAc-P
UDP-GlcNAc
UDP-MurNAc
UDP-MurNAc-dipeptide
d-ala-d-ala
IC/mg
Norm
HYP
HYP_PEP
c.
Van-BODIPY
DIC
Van-BODIPY + DIC
10 µm
Replication
Hypoxia
Hypoxia + PEP
d.
AMP
% Viability
W/O PEP
W/ PEP
Hypoxia time (Days)

**S Fig. 7. The effect of exogenous PEP on hypoxic Mtb PG biosynthesis**. (**a**) Schematic depicting Mtb PG lipid I biosynthesis pathway and MurA step at which PEP is a substrate. G6P, glucose phosphate; GlcNAc-P, N-acetyl glucosamine phosphate; UDP-GlcNAc; UDP-N-acetyl glucosamine; UDP-MurNAc, UDP-N-acetyl muramic acid; PEP, phosphoenolpyruvate. (**b**) Intrabacterial pool sizes of PG pathway precursors, incubated in acetate medium for 24 hrs at 20% $O_2$ (Norm), 1% $O_2$ (HYP) and 1% $O_2$ with PEP supplementation (HYP_PEP). Total bar heights indicate the intrabacterial pool sizes detected by LC-MS ion counts (IC) and normalized to biomass. All values are the average of two independent biological triplicates ± SEM. *, $P<0.01$ by Student's unpaired t-test. (**c**) Confocal fluorescence microscopy images of Mtb in NORM, HYP, or HYP_PEP states stained with Van-BODIPY to visualize nascent PG synthesis. DIC, differential interference contrast image. (**d**) CFU viability kinetics of hypoxic Mtb with or without PEP after treatment with 10X MIC equivalent ampicillin. All values are the average of three biological replicates ± SEM. *, $P<0.005$ by ANOVA with Bonferroni post-test correction.

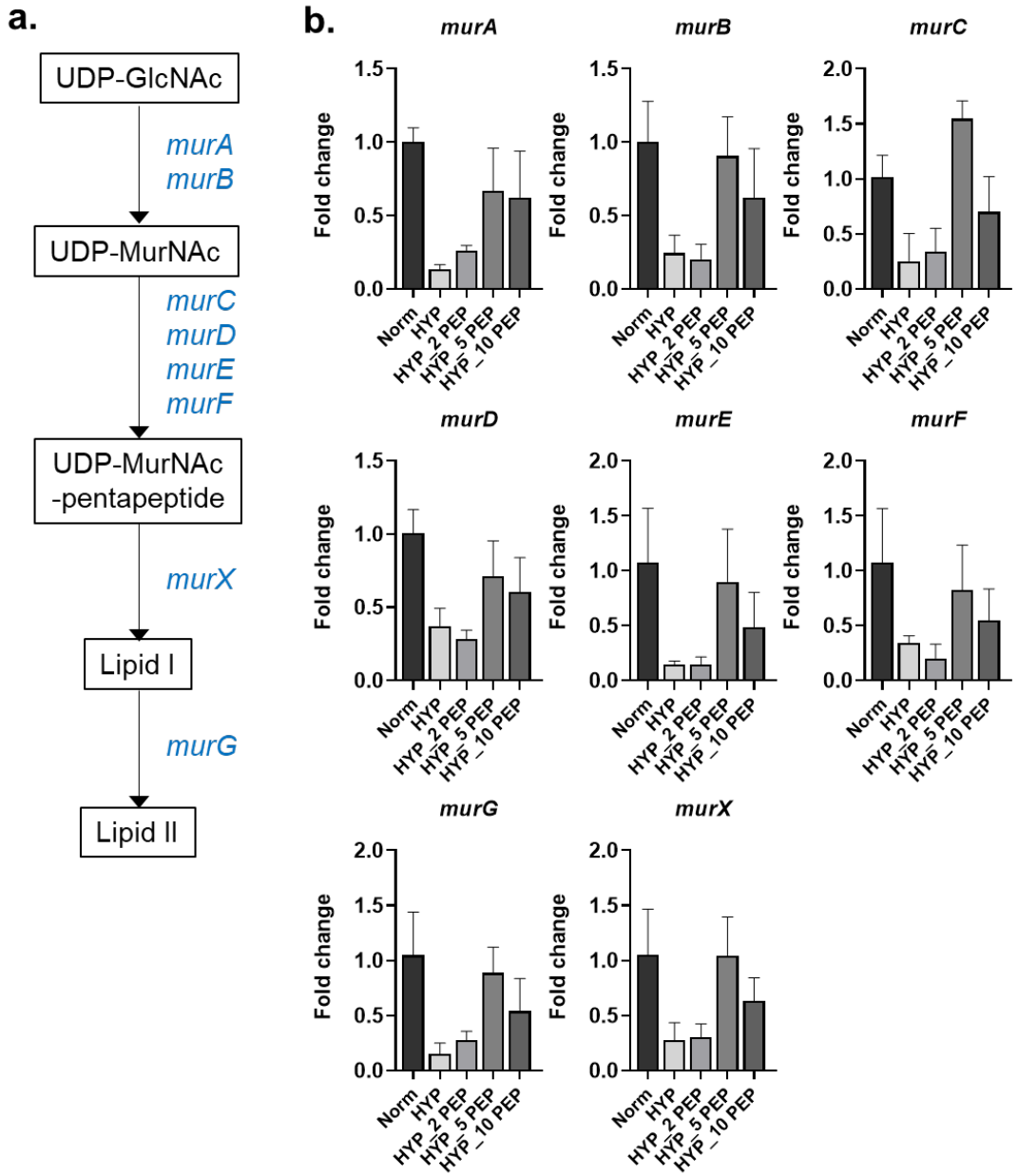


**S Fig. 8. The effect of exogenous PEP on hypoxic Mtb PG biosynthesis pathway gene mRNA expression**. (**a**) Schematic depicting Mtb PG biosynthesis pathway and genes involved in each step. Abbreviations are as in Fig. S6a. (**b**) PG biosynthesis pathway gene transcript levels following incubation for 24 hrs at 20% $O_2$ (Norm), 1% $O_2$ (HYP), and 1% $O_2$ with 2, 5, or 10 mM PEP (HYP_2 PEP, HYP_5 PEP or HYP_10 PEP).

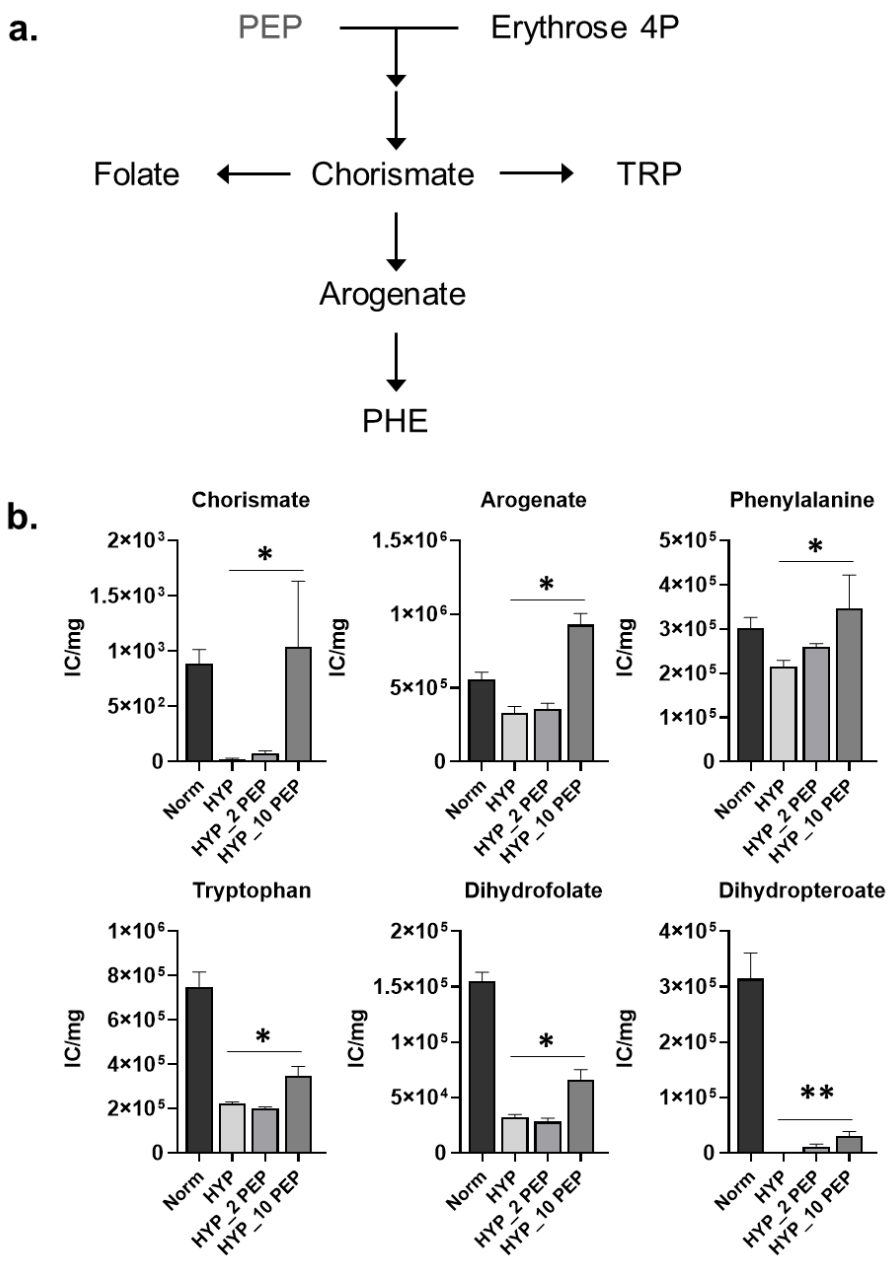


**S Fig. 9. The effect of exogenous PEP on hypoxic Mtb shikimate pathway**. (**a**) Schematic depicting Mtb shikimate pathway and its interconnected downstream pathways including aromatic amino acid pathways and folate metabolism pathways. (**b**) Intrabacterial pool sizes of select intermediates in the shikimate pathway and downstream pathways of Mtb incubated at 20% $O_2$ (Norm), 1% $O_2$ (HYP), and 1% $O_2$ in the presence of 2 or 10 mM PEP (HYP_2 PEP or HYP_10 PEP). Total bar heights indicate the intrabacterial pool sizes detected by LC-MS ion counts (IC) and normalized to biomass. All values are the average of three biological replicates ± SEM. *, P<0.01; **, P<0.05 by Student's unpaired t-test.

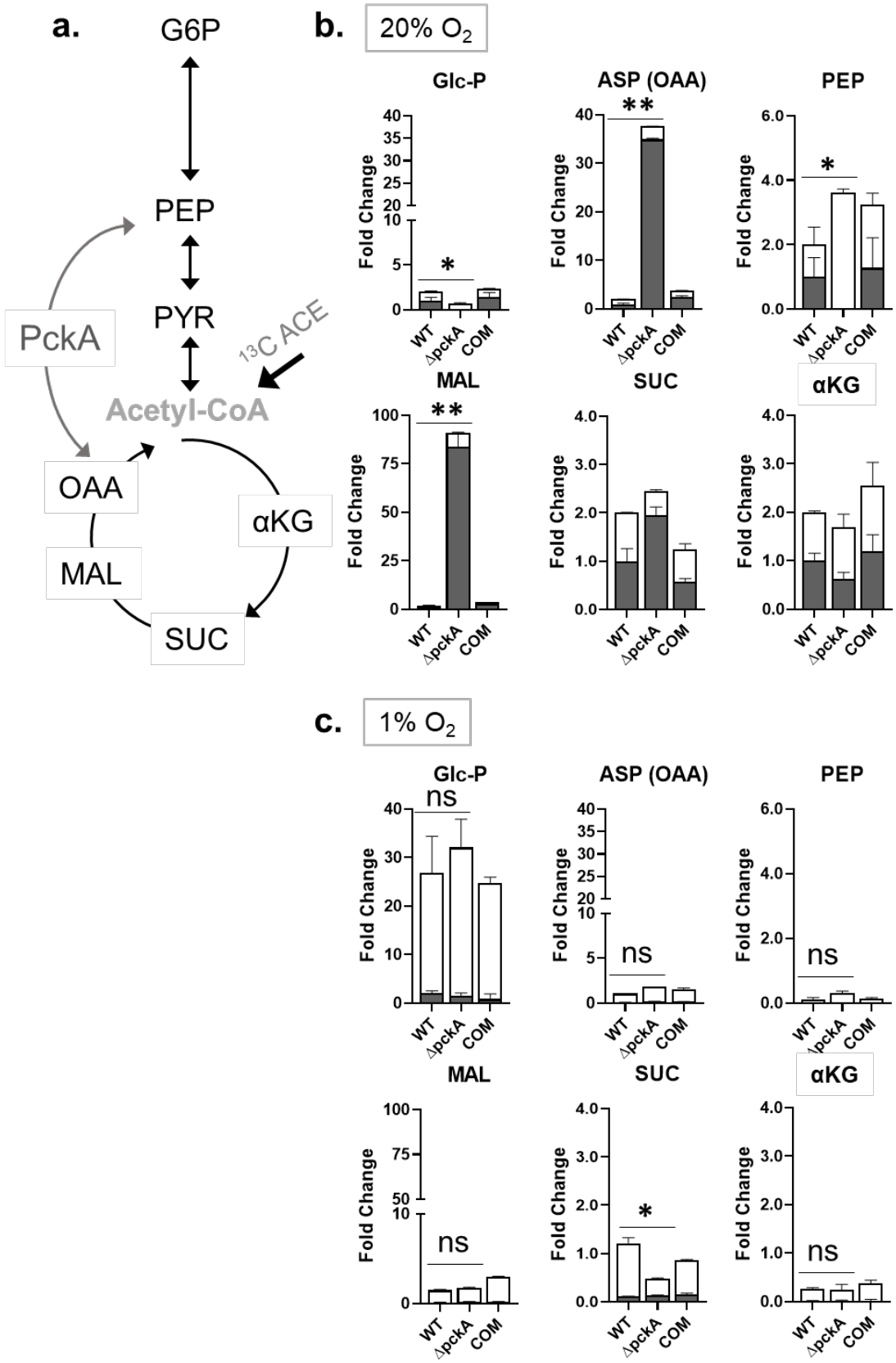
a.
G6P
PEP
PYR
PckA
13C ACE
Acetyl-CoA
OAA
αKG
MAL
SUC
b.
20% O2
Glc-P
ASP (OAA)
PEP
MAL
SUC
αKG
Fold Change
WT
ΔpckA
COM
c.
1% O2
ns

**S Fig. 10. The effect of PckA deficiency on hypoxic Mtb metabolic networks**. (**a**) Schematic depicting Mtb CCM including glycolysis and the TCA cycle. PckA catalytic activity is denoted by a gray arrow. Intrabacterial pool sizes and $^{13}C$ enrichment of CCM intermediates of Erdman WT, *pckA* deficient Mtb (ΔpckA), and ΔpckA complemented with *pckA* (COM) incubated in [U-$^{13}C$] acetate containing media for 24 hrs at 20% $O_2$ (**b**) or 1% $O_2$ (**c**). Abbreviations are as in Figure 2a. All values are the average of three biological replicates ± SEM. *, P<0.01; ns, not significant by Student's unpaired t-test.

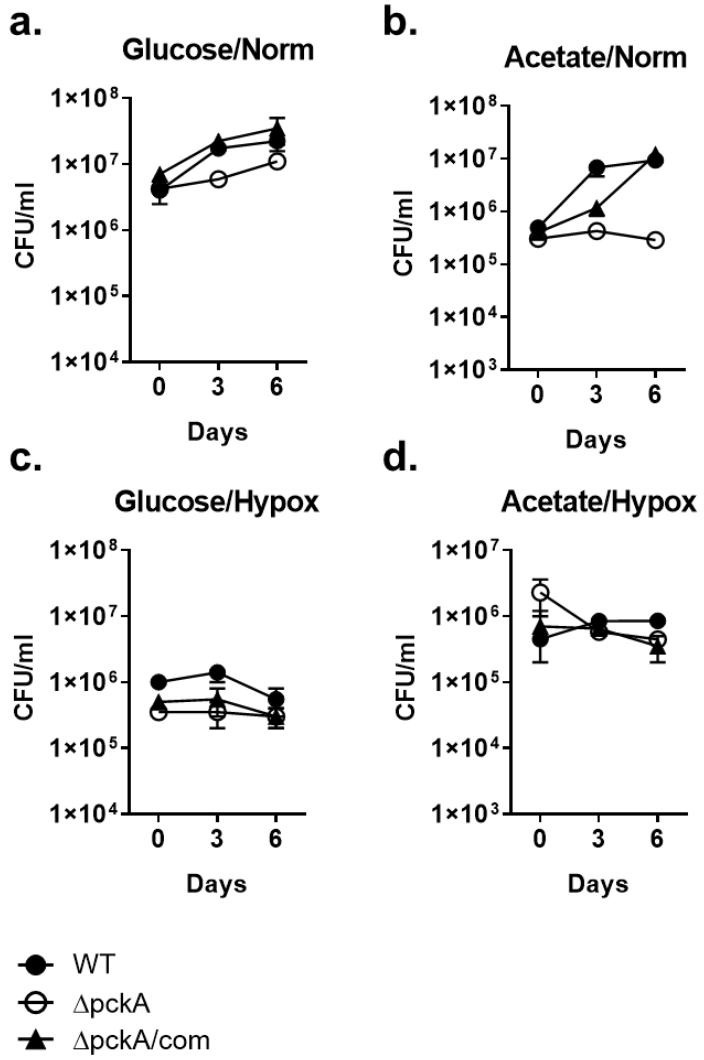


**S Fig. 11. Functional essentiality of PckA for Mtb viability under hypoxia**. CFU viability of Erdman WT, *pckA* deficient Mtb (ΔpckA), and ΔpckA complemented with *pckA* (ΔpckA/com) incubated at 20% $O_2$ at days 0, 3, and 6 in the presence of 0.2% glucose (**a**) or 0.2% acetate (**b**). CFU viability of WT, ΔpckA, and ΔpckA/com incubated at 1% $O_2$ in the presence of 0.2% glucose (**c**) or 0.2% acetate (**d**).

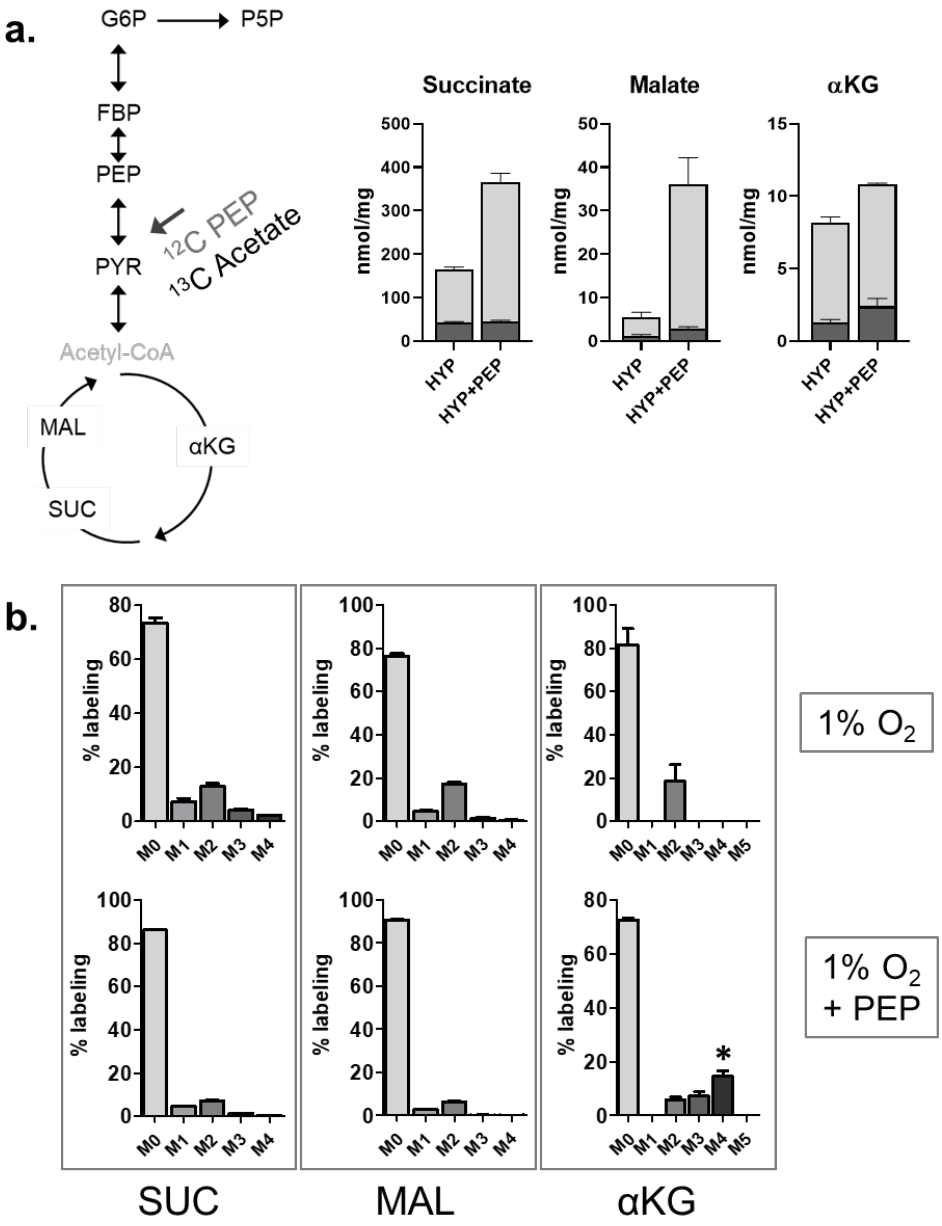
a.
G6P
P5P
FBP
PEP
PYR
12C PEP
13C Acetate
Acetyl-CoA
MAL
αKG
SUC
Succinate
Malate
αKG
nmol/mg
HYP
HYP+PEP
b.
% labeling
M0
M1
M2
M3
M4
M5
1% O2
1% O2 + PEP
SUC
MAL
αKG

**S Fig. 12. The effect of exogenous PEP on the isotopologue profile of hypoxic Mtb TCA cycle intermediates**. Mtb was incubated in [U-$^{13}$C] acetate media for 24 hrs at 1% $O_2$ in the presence or absence of 10 mM PEP. (**a**) Schematic depicting the Mtb CCM. [U-$^{13}$C] acetate was used as a carbon source. Abbreviations are as in Figure 2a. The effect of PEP supplementation on hypoxic Mtb TCA cycle intermediate (succinate, malate and αKG) abundance and $^{13}$C enrichment derived from exogenous $^{13}$C acetate. (**b**) Individual $^{13}$C isotopologue abundance of succinate, malate, and αKG expressed as a percentage relative to the total abundance of all ion species (labeled and unlabeled). Isotopologue composition of the metabolites at 1% $O_2$ in the presence of PEP was included. M0, unlabeled; M1, singly $^{13}$C labeled; M2, doubly $^{13}$C labeled and so on. * in 1% $O_2$+PEP indicates $^{13}C_4$ labeled species of αKG, which is indicative of incorporation of multiple acetate units arising from canonical TCA cycle activity. At 1% $O_2$ with no PEP, the M2 isotope species is major which is indicative of incorporation of a single acetate unit.

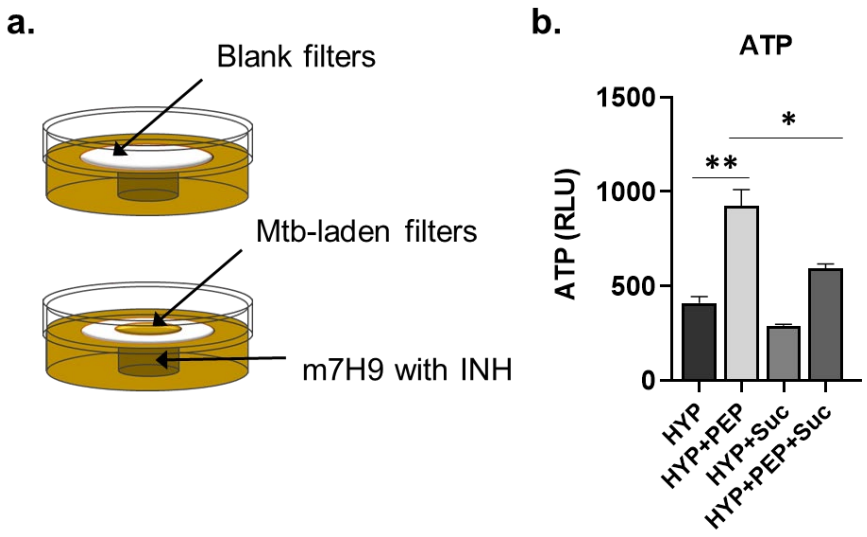


**S Fig. 13.** (**a**) Schematic illustrating the device used to measure antibiotic uptake. This was used to make timed start-stop measurements of remaining antibiotics in the media within the plastic inlet. No bacterial filters were used as a negative control (no uptake level). (**b**) Intrabacterial ATP of Mtb incubated for 24 hrs at 1% $O_2$ (HYP), 1% $O_2$ with 10 mM PEP (HYP+PEP), 1% $O_2$ with 2 mM succinate (HYP+Suc), and 1% $O_2$ with both PEP and succinate (HYP+PEP+Suc). Supplementing succinate to the culture medium was used as a functional means of inhibiting secretion of intrabacterial succinate. All values are the average of three biological replicates ± SEM. *, $P<0.01$; ns, not significant by Student's unpaired t-test.

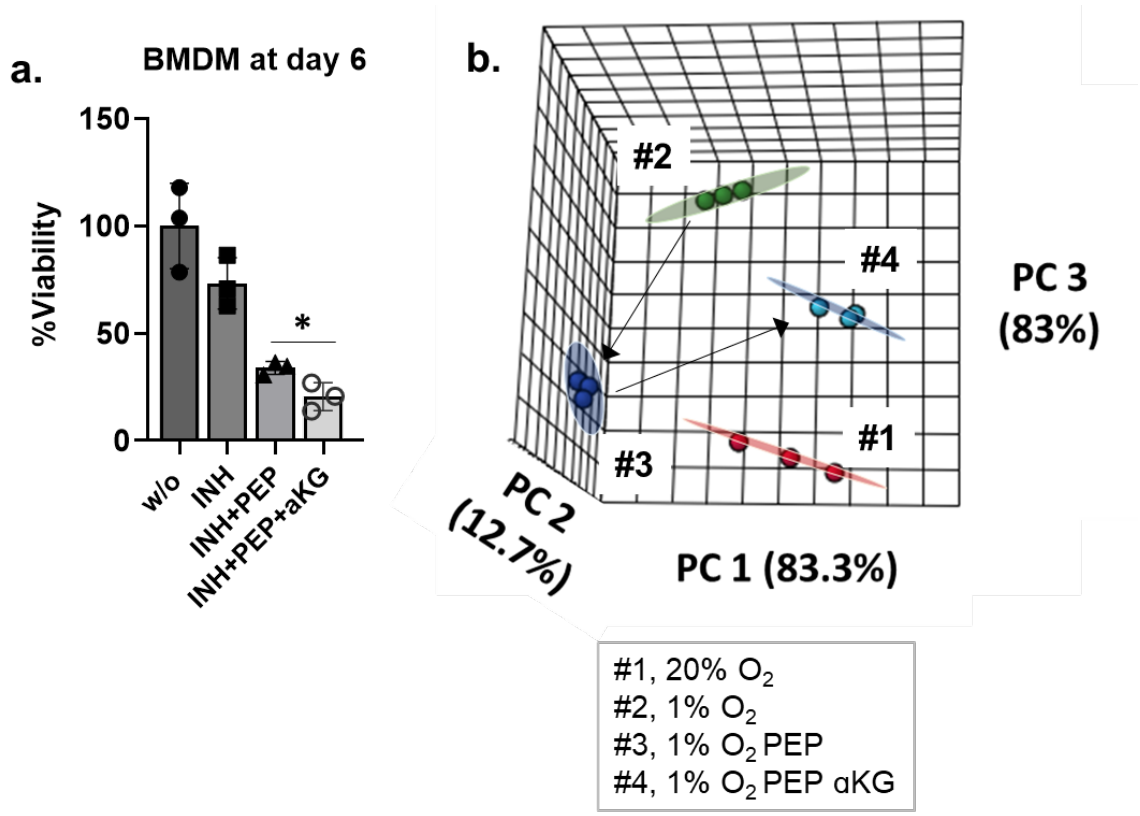


**S Fig. 14. The synergy of αKG with PEP mediated metabolic restoration of hypoxic Mtb**. (**a**) The viability of intracellular Mtb using mouse bone marrow derived macrophages pretreated with αKG and/or PEP. The CFU viability of intracellular Mtb against 10X MIC INH was monitored. (**b**) 3D principal component analysis plot of the Mtb metabolome pattern under 20% $O_2$ (#1, red dots), 1% $O_2$ (#2, green dots), 1% $O_2$ with PEP (#3, blue dots), and 1% $O_2$ with PEP and αKG (#4, light blue dots).

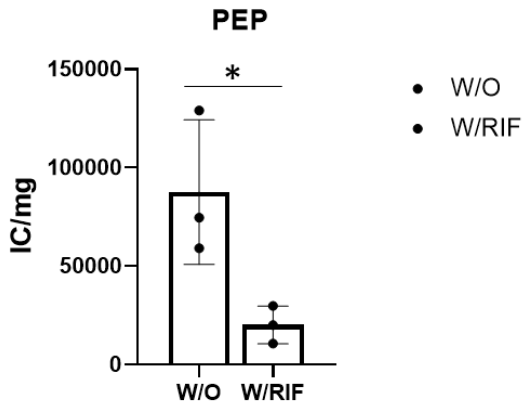


**S Fig. 15. PEP abundance in *M. smegmatis* after treatment with 1X MIC RIF**. *M. smegmatis* downregulated the PEP abundance in response to 1-day incubation with 1X MIC RIF. PEP was detected using LC-MS metabolomics. All values are the average of three biological replicates ± SEM. *, P<0.01 by Student's unpaired t-test.

**a.**

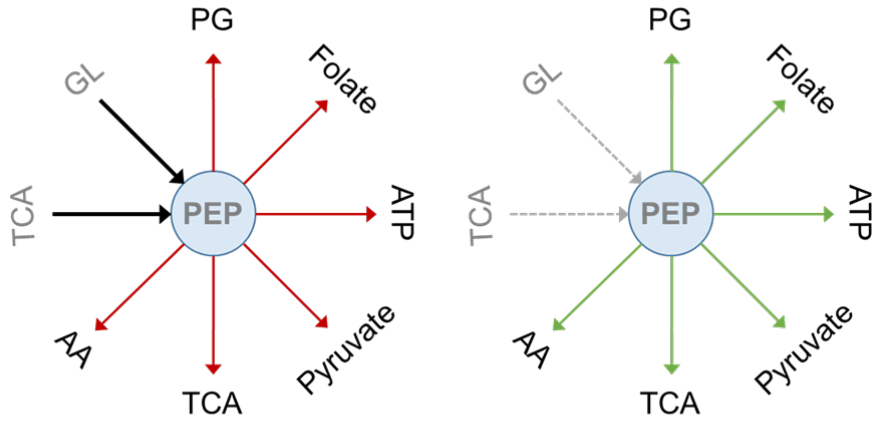


Replicating state NR state

**b.**

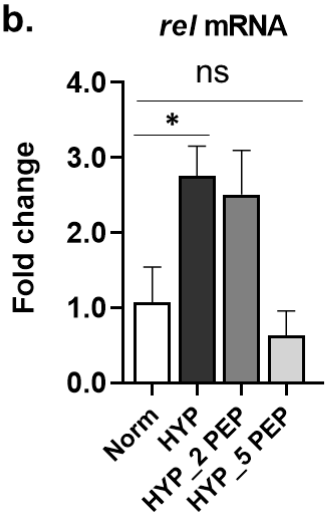

**S Fig. 16. Metabolic networks of NR Mtb related to PEP biosynthesis and consumption**. (**a**) PEP depletion in hypoxic Mtb causes remodeling of metabolic networks required for the NR Mtb phenotypic shift. In the replicating stage, Mtb activates glycolytic and gluconeogenic carbon flux towards the biosynthesis of PEP to continuously replenish multiple downstream metabolic networks (left panel). In the NR state under hypoxia or drug treatment, Mtb downregulates glycolytic and gluconeogenic carbon fluxes towards the biosynthesis of PEP to functionally limit multiple downstream metabolic networks (right panel). Black solid arrows and red arrows, the greater activities; gray dotted arrows and green arrows, downregulated activities. (**b**) mRNA expression levels of Mtb *rel* following incubation for 24 hrs under 20% $O_2$ (Norm), 1% $O_2$, (HYP), 1% $O_2$ with 2 mM PEP (HYP_2 PEP) or 5 mM PEP (HYP_5 PEP). All values are the average of three biological replicates ± SEM. *, $P<0.01$; ns, not significant by Student's unpaired t-test.

**Table S1. Metabolites significantly changed in hypoxia compared with normoxia.**

| | Metabolites | Fold Change (FC) | log2(FC) | raw.pval | -log10(p) |
|---|---|---|---|---|---|
| **Down-regulated metabolites** | PEP | 0.0067229 | -7.2167 | 0.003379 | 2.4712 |
| | 3-Sulfomuconate | 0.018942 | -5.7222 | 0.005261 | 2.2789 |
| | 4-Methylene-L-glutamine | 0.021298 | -5.5532 | 8.84E-06 | 5.0535 |
| | Citrulline | 0.026575 | -5.2338 | 3.71E-08 | 7.4311 |
| | 5-Hydroxyisourate | 0.026949 | -5.2136 | 0.00415 | 2.382 |
| | Glutamine | 0.039631 | -4.6572 | 3.6E-06 | 5.4438 |
| | L-Citrulline | 0.043123 | -4.5354 | 2.1E-05 | 4.6775 |
| | 2-Oxoglutarate | 0.044688 | -4.484 | 6.08E-05 | 4.216 |
| | alpha-ketoglutarate | 0.044726 | -4.4828 | 6.42E-05 | 4.1926 |
| | 3-Propylmalate | 0.044856 | -4.4786 | 5.76E-05 | 4.2399 |
| | 5'-Methylthioadenosine | 0.049243 | -4.3439 | 2.64E-05 | 4.5785 |
| | Phosphoenolpyruvate | 0.059713 | -4.0658 | 0.009984 | 2.0007 |
| | D-Glutamine | 0.063321 | -3.9812 | 6.63E-05 | 4.1784 |
| | D-Glycerate | 0.066428 | -3.9121 | 0.000321 | 3.4931 |
| | UDP-glucose | 0.072835 | -3.7792 | 4.73E-07 | 6.3248 |
| | Nicotinate | 0.082904 | -3.5924 | 9.52E-06 | 5.0215 |
| | N-Acetylornithine | 0.089195 | -3.4869 | 2.6E-05 | 4.5855 |
| | 3-Phospho-D-glyceroyl phosphate | 0.094867 | -3.3979 | 0.022032 | 1.6569 |
| | Glycerate | 0.10311 | -3.2777 | 0.000414 | 3.3828 |
| | Indolepyruvate | 0.10361 | -3.2707 | 1.39E-05 | 4.8572 |
| | D-Alanyl-D-alanine | 0.10829 | -3.2071 | 1.24E-05 | 4.9071 |
| | Anthranilate | 0.12831 | -2.9623 | 1.13E-05 | 4.9481 |
| | 1-Ribosylimidazole-4-acetate | 0.18826 | -2.4092 | 0.000849 | 3.0711 |
| | Rhodomycin D | 0.23105 | -2.1137 | 4.69E-05 | 4.3289 |
| | 2-Phosphinomethylmalate | 0.24878 | -2.007 | 0.0002 | 3.6993 |
| | gamma-L-Glutamyl-L-cysteine | 0.2783 | -1.8453 | 5.91E-05 | 4.2282 |
| | L-Tryptophan | 0.2896 | -1.7879 | 0.000161 | 3.7945 |
| | 2-Methylcitrate | 0.29606 | -1.7561 | 7.08E-05 | 4.1501 |
| | DL--Lipoic Acid | 0.29654 | -1.7537 | 6.57E-05 | 4.1822 |
| | Methyl Citrate | 0.29654 | -1.7537 | 6.57E-05 | 4.1822 |
| | 2,4-Bisacetamido-2,4,6-trideoxy-beta-L-altropyranose | 0.31806 | -1.6526 | 8.13E-05 | 4.0901 |
| | Pyruvate | 0.36009 | -1.4736 | 0.000181 | 3.7415 |
| | 6Z,9Z,12Z,15Z,18Z,21Z-3-Oxotetracosahexa-6,9,12,15,18,21-enoyl-CoA | 0.37736 | -1.406 | 0.000203 | 3.6924 |
| | L-Serine | 0.37851 | -1.4016 | 0.000146 | 3.8364 |
| | Glutarate | 0.38398 | -1.3809 | 0.000213 | 3.6706 |

| | | | | | |
|---|---|---|---|---|---|
| | L-Alanine | 0.40096 | -1.3185 | 0.000119 | 3.9235 |
| | L-Valine | 0.41535 | -1.2676 | 0.000217 | 3.6636 |
| | N2-Succinyl-L-ornithine | 0.42129 | -1.2471 | 0.0001 | 3.9993 |
| | L-Proline | 0.42303 | -1.2412 | 0.000101 | 3.9976 |
| | Geranyl diphosphate | 0.43069 | -1.2153 | 7.98E-06 | 5.0982 |
| | N-Methyl-L-glutamate | 0.524 | -0.93237 | 2.28E-05 | 4.6427 |
| | N-Succinyl-LL-2,6-diaminoheptanedioate | 0.56623 | -0.82054 | 0.000669 | 3.1747 |
| | Thiamine acetic acid | 0.57048 | -0.80975 | 7.91E-07 | 6.1017 |
| | D-Leucine | 0.61119 | -0.7103 | 0.001467 | 2.8336 |
| | Prunasin | 0.63446 | -0.6564 | 0.001045 | 2.9807 |
| | Glutamate | 0.63568 | -0.65363 | 9.55E-05 | 4.0202 |
| | L-Glutamate | 0.63568 | -0.65363 | 9.55E-05 | 4.0202 |
| | R-S-Lactoylglutathione | 0.64131 | -0.6409 | 0.000289 | 3.5389 |
| | N-Succinyl-L-citrulline | 0.64214 | -0.63905 | 0.004631 | 2.3343 |
| | L-Threonine | 0.64358 | -0.63581 | 0.000547 | 3.2622 |
| | Erythromycin B | 0.64867 | -0.62444 | 0.000353 | 3.452 |
| | 2',3'-Cyclic AMP | 0.65758 | -0.60477 | 0.000159 | 3.7998 |
| | 4-Aminobutanoate | 0.666 | -0.58641 | 0.000532 | 3.2742 |
| | GABA | 0.666 | -0.58641 | 0.000532 | 3.2742 |
| **Up-regulated metabolites** | Maltose | 1.5055 | 0.59022 | 8.63E-05 | 4.0641 |
| | Cyclohexylamine | 1.5145 | 0.59888 | 0.006082 | 2.216 |
| | 3,6-Dihydronicotinic acid | 1.5403 | 0.62317 | 0.00067 | 3.1737 |
| | 4-Sulfobenzyl alcohol | 1.586 | 0.66543 | 0.000329 | 3.4822 |
| | 34a-Deoxy-rifamycin W | 1.5925 | 0.67126 | 0.00475 | 2.3233 |
| | sn-Glycero-3-phosphoethanolamine | 1.6036 | 0.68131 | 0.000126 | 3.8993 |
| | N-Methylpelletierine | 1.6301 | 0.70496 | 0.034357 | 1.464 |
| | Yersiniabactin | 1.6493 | 0.72184 | 0.00064 | 3.1938 |
| | PG160/1819Z | 1.6924 | 0.75907 | 0.000159 | 3.7983 |
| | Histidine | 1.8914 | 0.91945 | 0.00025 | 3.6016 |
| | R-Lactate | 1.9007 | 0.92655 | 0.023307 | 1.6325 |
| | PE160/1819Z | 2.0062 | 1.0045 | 0.00283 | 2.5482 |
| | L-Histidine | 2.0448 | 1.0319 | 0.000145 | 3.838 |
| | 1-Palmitoyl Lysophosphatidic Acid | 2.0504 | 1.0359 | 0.001815 | 2.7412 |
| | Orthophosphate | 2.0709 | 1.0502 | 1.55E-05 | 4.8111 |
| | 2-Amino-4,6-dinitrotoluene | 2.0738 | 1.0523 | 0.001043 | 2.9815 |
| | Nitrate | 2.093 | 1.0656 | 0.02532 | 1.5965 |
| | Aquayamycin | 2.3096 | 1.2076 | 0.000124 | 3.9076 |
| | N-Acetyl-L-glutamate | 2.3291 | 1.2198 | 0.000111 | 3.954 |
| | D-Glucono-1,5-lactone | 2.5213 | 1.3342 | 0.000235 | 3.6297 |
| | beta-D-Glucosamine | 2.6412 | 1.4012 | 0.004806 | 2.3182 |
| | meso-2,6-Diaminoheptanedioate | 3.1221 | 1.6425 | 3.36E-05 | 4.4742 |

| | | | | | |
|---|---|---|---|---|---|
| | Propanoate | 3.3318 | 1.7363 | 0.00016 | 3.7956 |
| | Xanthoxic acid | 3.6354 | 1.8621 | 0.035445 | 1.4504 |
| | Succinate | 4.5303 | 2.1796 | 0.000493 | 3.3067 |
| | L-Ornithine | 4.8254 | 2.2707 | 5.64E-05 | 4.2491 |
| | Ectoine | 4.8807 | 2.2871 | 2.65E-06 | 5.576 |
| | 2-C-Methyl-D-erythritol 4-phosphate | 5.039 | 2.3331 | 0.001075 | 2.9684 |
| | 3-Ethylmalate | 6.8281 | 2.7715 | 0.000941 | 3.0263 |
| | Triose P | 7.5388 | 2.9143 | 0.000155 | 3.8105 |
| | Glycerone phosphate | 7.6026 | 2.9265 | 0.000146 | 3.8347 |
| | L-Galactonate | 7.8319 | 2.9694 | 0.000303 | 3.5189 |
| | 1,7-Dimethyluric acid | 7.8418 | 2.9712 | 0.000301 | 3.5215 |
| | dTMP | 8.4778 | 3.0837 | 1.84E-08 | 7.7354 |
| | Adenosine | 8.9317 | 3.1589 | 5.09E-05 | 4.2932 |
| | L-Galactose | 11.997 | 3.5846 | 0.000309 | 3.5105 |
| | Theophylline | 13.337 | 3.7374 | 0.000365 | 3.4382 |
| | 5-Acetylamino-6-formylamino-3-methyluracil | 13.948 | 3.802 | 0.000776 | 3.1099 |
| | Glucose | 14 | 3.8073 | 0.000308 | 3.5111 |
| | Acetone cyanohydrin | 14.25 | 3.8329 | 6.22E-06 | 5.2061 |
| | UMP | 14.607 | 3.8686 | 1.24E-07 | 6.9061 |
| | sn-Glycerol 1-phosphate | 22.479 | 4.4905 | 3.74E-05 | 4.427 |
| | AMP | 23.793 | 4.5725 | 0.000143 | 3.8441 |
| | Pseudouridine 5'-phosphate | 30.221 | 4.9175 | 3.13E-06 | 5.5051 |
| | L-Ribulose 5-phosphate | 30.385 | 4.9253 | 6.29E-06 | 5.201 |
| | Pentose 5 phosphate | 30.385 | 4.9253 | 6.29E-06 | 5.201 |
| | Acetyl phosphate | 39.525 | 5.3047 | 0.01669 | 1.7776 |
| | Hypoxanthine | 50.064 | 5.6457 | 0.000188 | 3.7264 |
| | CMP | 53.214 | 5.7337 | 1.32E-08 | 7.8781 |
| | GMP | 60.609 | 5.9215 | 3.52E-07 | 6.453 |
| | Pantetheine 4'-phosphate | 81.688 | 6.3521 | 5.55E-06 | 5.2561 |
| | N1-5-Phospho-alpha-D-ribosyl-5,6-dimethylbenzimidazole | 87.592 | 6.4527 | 5.59E-06 | 5.2528 |
| | Trehalose | 118.5 | 6.8887 | 1.04E-06 | 5.981 |
| | UWM6 | 118.5 | 6.8887 | 1.04E-06 | 5.981 |
| | 2-alpha-D-Mannosyl-3-phosphoglycerate | 126.76 | 6.986 | 1.04E-06 | 5.9848 |
| | IMP | 134.94 | 7.0762 | 1.06E-06 | 5.9733 |
| | Selenodiglutathione | 207.34 | 7.6959 | 0.000248 | 3.6055 |
| | Macarpine | 222.53 | 7.7979 | 0.001794 | 2.7461 |
| | Hexose 6 phosphate | 240.76 | 7.9114 | 0.000611 | 3.214 |
| | D-Hexose 6-phosphate | 245.26 | 7.9382 | 0.000616 | 3.2105 |
| | cis,cis-3,6-Dodecadienoyl-CoA | 247.62 | 7.952 | 0.000141 | 3.8503 |

| | | | | | |
|---|---|---|---|---|---|
| | N-Acetyl-D-glucosamine 6-phosphate | 459.77 | 8.8448 | 1.18E-06 | 5.9276 |
| | Sedoheptulose 7-phosphate | 500.63 | 8.9676 | 0.000774 | 3.1112 |
| | UDP-L-rhamnose | 1659.7 | 10.697 | 0.000291 | 3.5354 |

**Table S2. qRT-PCR primers**

| | Name | Sequence (5' - 3') |
|---|---|---|
| **1** | *pckA*-F | GATGAATGGCGTCAGGAACT |
| | *pckA*-R | GGGCGTCGAACTCATCTTT |
| **2** | *murA*-F | GCGGAGATTCAGTTGGAGTT |
| | *murA*-R | TCGAGCCGCATTGTGAATAG |
| **3** | *murB*-F | TGCTGGTGGCTCCAATTT |
| | *murB*-R | CGATGGTGATGCCGCTATT |
| **4** | *murC*-F | GGAATTCGAGTGCTGCGATA |
| | *murC*-R | CTGAGGCCAACCGGATATG |
| **5** | *murD*-F | CCCAGTCGTTCAGGTTGTG |
| | *murD*-R | CTCACCGGCTTTGTCATCTT |
| **6** | *murE*-F | GCGCCTTCACCAATCTCT |
| | *murE*-R | AGTCCGGATCGAACAATGAC |
| **7** | *murF*-F | CGCACCGACTACCTGATTT |
| | *murF*-R | GAGCCGAACTCACCCAAA |
| **8** | *murX*-F | GCCCTTCCACCACCATTT |
| | *murX*-R | GCCACTCACCGTAGAACAAG |
| **9** | *murG*-F | GACGGTCGCCGAAGTATC |
| | *murG*-R | TACCGGCAACGCATTCA |
| **10** | *relA*-F | CGGAGAAGTTGTCGAGGTTT |
| | *relA*-R | CTGGCGGATCTTCGTCTTT |
| **11** | *sigA*-F | ACGAAGACCACGAAGACCTCGAA |
| | *sigA*-R | GTAGGCGCGAACCGAGTCGGCGG |
| **12** | Glucokinase-F | TTGATACCCAACACCGAGTTC |
| | Glucokinase-R | TGGATAGGTCCAGTCGTTCT |
| **13** | Phosphohexose isomerase-F | GGACTGTGGTACTCCAATTTCT |
| | Phosphohexose isomerase-R | ATGGTCAACTGCTGAAGGTAG |
| **14** | Phosphofructokinase-F | TGCGGATTGGAGTTCTTACC |
| | Phosphofructokinase-R | GCGAAAGCCGTTCTGAAATC |
| **15** | Aldolase-F | CGGAGTTCACCCACGTTATC |
| | Aldolase-R | TAGCTGTCCAACTTGTCCTTG |
| **16** | G3PDH-F | GGAGTTAACGACGACAAGTATGA |
| | G3PDH-R | TCATCGTCGAGCACTTTGG |
| **17** | Phosphoglycerate kinase-F | CTGCTGGAAGACGACATGAT |
| | Phosphoglycerate kinase-R | ACTTCTCCGTGACCACTAGAT |
| **18** | Phosphoglycerate mutase-F | GAGTTCAACGCCACCTACA |
| | Phosphoglycerate mutase-R | GGCAGATAACGATCCAGGAC |
| **19** | Enolase-F | CCACTGTCCGAAGACGATTG |
| | Enolase-R | TCGGGATTGGTGACAAAGATG |
| **20** | Pyruvate kinase-F | CGGAAGCCATCGACAATCT |
| | Pyruvate kinase-R | TACCAGCGGGACCTCTT |